J. Physiol. (1979), **287**, *pp.* 163–176
With 6 text-figures
Printed in Great Britain

RELATIONSHIP BETWEEN SPATIAL FREQUENCY SELECTIVITY AND RECEPTIVE FIELD PROFILE OF SIMPLE CELLS

BY BRYAN W. ANDREWS AND DANIEL A. POLLEN

From the Neurobiology Laboratory, Neurosurgical Service, Massachusetts General Hospital, Boston, Massachusetts 02114, U.S.A.

(*Received 31 March 1978*)

SUMMARY

1. Receptive fields of simple cells in area 17 of the cat were mapped with stationary stimuli. Spatial frequency selectivities of the same cells were measured with drifting sinusoidal gratings.

2. The reconstructed field profile (inverse Fourier transform of selectivity curve) shows qualitative agreement with the mapped profile, and suggests the existence of additional side-lobes in the field. The side-lobes may correspond to the 'unresponsive regions' investigated by Maffei & Fiorentini (1976).

3. Our data suggest that the simple cell may perform approximately linear spatial summation of inputs to the visual system. However, the output of the simple cell is generally non-linear as reflected in its truncated responses to gratings.

INTRODUCTION

Simple cells in cortical area 17 of the cat were defined by Hubel & Wiesel (1962) as having receptive fields composed of distinct excitatory and inhibitory regions which show response summation within a region and antagonism between regions. Campbell, Cooper & Enroth-Cugell (1969) measured the spatial frequency selectivity of cortical cells without distinguishing cell type. Maffei & Fiorentini (1973) used sinusoidal gratings presented at constant velocity to show that both bipartite and tripartite simple cells have spatial frequency selectivity curves with full width at half-maximal amplitude of approximately 1·0 octave. The preferred spatial frequencies of simple cells in their studies spanned the range 0·2–2·0 cycles per degree.

In further studies using drifting sinusoidal gratings, Maffei & Fiorentini (1976) investigated the influence on the simple cell's response of large 'unresponsive regions' flanking the classically mapped receptive field. They found that these regions, unresponsive to localized stimuli, can dramatically facilitate or inhibit the cell's responses to stimuli in the classical field. Moreover, the 'unresponsive regions' exhibit spatial frequency selectivity matched to the selectivity of the classical portion of the field. Bishop, Henry & Smith (1971) observed subliminal excitatory fringes in many simple cell fields, using a moving bar whose effect through one eye facilitated its effect through the other.

Our objective is to examine the relationship between the simple cell's receptive field profile and its spatial frequency selectivity. We used stationary narrow bars of light to establish the positions and sizes of the excitatory and inhibitory regions of

each cell's receptive field, and drifting sinusoidal gratings to measure the spatial frequency selectivity of the cell. While neither of these steps alone was novel, we felt that both were necessary so that a comparison of field profile and spatial frequency selectivity could be made for individual cells.

What relationship might be expected to exist between a simple cell's field profile and its spatial frequency selectivity? One possibility is that the cell performs linear spatial summation. In this case, the cell's response to a sinusoidal input, as a function of spatial frequency, is the Fourier transform of the cell's field profile. We test this hypothesis by comparing the inverse Fourier transform of each cell's selectivity curve (the *reconstructed field profile*) directly with the cell's *mapped field profile*. We chose this technique rather than comparing the forward transform of the mapped profile with the selectivity curve because of difficulties in obtaining a quantitative mapped profile, as will be explained in Methods.

Reconstructed field profile

The reconstruction of a cell's field profile from its spatial frequency selectivity curve was based on certain assumptions:

(1) the field contains no component at zero spatial frequency. This is equivalent to the statement that the total of excitation and inhibition across the field is zero, and corresponds to the failure of the cell to respond to uniform illumination, as first observed by Hubel & Wiesel (1962):

(2) the response of the simple cell to a drifting sinusoidal grating has the form of a truncated sinusoid (Movshon & Tolhurst, 1975; see our Fig. 1). The truncation may be a non-linearity arising at the output of the simple cell itself. The directional selectivity of most simple cells implies an additional non-linearity in the processing of afferents to the simple cell. We assume that both of these non-linear processes may be distinct from the process of integration occurring post-synaptically within the simple cell. It is the linearity of this latter process which will be tested by the comparison of mapped and reconstructed field profiles. This assumption that known non-linearities may be separable from some other possibly linear stages of the system is consistent with the finding of Movshon & Tolhurst (1975) that simple cell responses to drifting sinusoids depend linearly on stimulus contrast but display a non-linear output waveform.

(3) the phase used for each spatial frequency component in the reconstruction is taken directly from the phase of the cell's response to the drifting grating of that spatial frequency. This assumes that the latencies of the cell's responses to various spatial frequencies are equal. The assumption was tested with stationary gratings and was found to be valid.

METHODS

Preparation and recording

Sixteen adult cats were anaesthetized with halothane for tracheostomy and craniotomy, and were paralysed and maintained on nitrous oxide and oxygen (70%/30%) for analgesia and light anaesthesia during cell study; details appear elsewhere (Pollen & Ronner, 1975).

Activity of single neurones was recorded extracellularly with tungsten micro-electrodes (Hubel, 1957). We made electrode penetrations near Horsley–Clarke co-ordinates P3·0–P4·0 and L1·0–L2·0. We studied only simple cells in area 17 having receptive fields in the central 5° of visual space. Of twenty-five cells studied, sixteen yielded data suitable for the detailed analysis described here.

Visual stimulation

All stimuli were projected on a tangent screen 150 cm from the cat's eye. Bar images were obtained by projection through an adjustable mask, and gratings by projection through photographic transparencies. The latter were made by Drs Stromeyer and Lange (Stromeyer, Lange & Ganz, 1973), and were available in quarter-octave steps of spatial frequency. All stimuli were superimposed on a uniform background luminance of 15·2 cd/m^2. Bars were typically of resultant luminance 25 cd/m^2. Gratings were typically of resultant mean luminance 20–30 cd/m^2 and resultant contrast 0·1–0·2.

Field mapping

A cell's receptive field map depends somewhat on the stimulus used in mapping: stationary bar, drifting bar, drifting edge, etc. (Bishop, Coombs & Henry, 1971; Fries & Albus, 1976). We desired a stimulus which would reveal the influence of local portions of the field independent of neighbouring portions. We therefore chose the stationary bar. This stimulus has the further advantage that it is not necessary to select an arbitrary direction and velocity of movement.

We projected a stationary light bar in the field parallel to the cell's preferred orientation. The length of the bar (parallel to the preferred orientation) was always sufficient to span the entire field. An electric shutter was repeatedly opened and closed with stimuli of increasing widths in different positions. When a stimulus was found eliciting maximal excitation only at stimulus onset or only at offset, the stimulus was considered to be filling an *on-region* or an *off-region* respectively (maximal excitation was judged by listening to an audio monitor of the cell's activity). The procedure was carried out until all such regions contained in the field were revealed.

It was very difficult to obtain a quantitative map of a receptive field. Quantitative mapping, region by region, would involve repetitive stimulation with a narrow bar at many points in the field. However, subthreshold contributions of the weaker points in the field would be missed by a narrow bar, no matter how many repetitions of the stimulus were used, whereas they can make a noticeable contribution to the response to an incrementally widened bar. For this reason we accepted the qualitative map yielded by the region-filling technique described above.

Each simple cell was classified as sustained or transient by a technique modified after that of Ikeda & Wright (1974). If the response to a stationary light bar within an on-region exceeded spontaneous activity by 3 spikes/sec for more than 1 sec, the cell was considered sustained; if less than 1 sec, transient.

Sinusoidal grating studies

Because responses to stationary gratings are so critically dependent on position, we routinely used drifting gratings. We avoided the passage of the leading or trailing edge of a grating across a cell's receptive field by using an electric shutter, which caused the drifting grating to appear and disappear abruptly while filling the entire field. The regions outside the *ends* of the field (where stimuli enter and leave the field) were occupied by the grating for a distance of at least one-half and usually over one field-diameter beyond the field boundary. The regions to the *sides* of the field were not stimulated, being shielded by a mask on the transparency. The cell's response to the abrupt general increase in mean luminance at the shutter's opening was always minor and usually subsided within 200 msec. The portion of the cell's response containing this transient was never used in data processing.

In six experiments a small, fast, linear photocell was placed at a known position at the side of the receptive field during drifting grating studies. The position was chosen arbitrarily, but subject to the condition that it be sufficiently far from the centre of the field to avoid influencing the cell's responses. The photocell's output voltage was proportional to local stimulus luminance, and was a sinusoid of temporal frequency equal to that of the stimulus. This signal enabled us to know the spatial phase (or position) of the stimulus at any moment, and in particular at those moments when the simple cell's response was maximal.

To avoid ambiguity, studies involving series of gratings are named according to the parameter held constant, not a parameter varied. Constant-velocity studies and constant-temporal-frequency studies were performed. The value of the constant parameter of a study was qualitatively chosen to maximize response amplitude.

To avoid possible distortion of the over-all shape of a selectivity curve arising from slow changes in the state of the animal, gratings within each study were presented in random order.

Data processing

Autocorrelation. As will be described, the periodic responses of simple cells to drifting gratings were all of a very consistent shape, differing only by scale factors in time and amplitude. The autocorrelations of the responses are therefore also of a consistent shape, and can be used to measure the amplitudes of the responses. The autocorrelation is preferable for this purpose, since it is a much smoother function than the response itself.

The modulation amplitude of the response, M, is proportional to the square root of the modulation amplitude of its autocorrelation. This relationship is apparent in particular for a sinusoid, $A + B\cos(kx)$, whose autocorrelation is $A^2 + \frac{1}{2}B^2\cos(kx)$, and follows in general from the autocorrelation theorem. If the 99 bins of the average response histogram have the values $h(0), h(1), \ldots, h(98)$, then the autocorrelation of the response is generated by the formula

$$a(z) = \frac{1}{N}\sum_{n=c}^{c+N} h(n)h(n+z),$$

where N denotes a domain of the response containing an integral number of cycles. The difference between the first minimum and the first non-central maximum of $a(z)$ was taken as M^2. As with $h(n)$, M has the units spikes/sec.

Fourier transformation. The spatial frequency selectivity of a cell is reflected in the modulation amplitude, $M(s)$, as a function of spatial frequency (s, in cycles/degree). The quantity $M(s)$ is complex, its phase specifying the spatial phase of the drifting grating stimulus at the instant of maximal firing rate. This is the instant at which the stimulus was superimposed on what may mathematically be considered as the equivalent spatial frequency component of the field profile. A typical phase function derived in this manner is shown in Fig. 2*B*. From the complex function $M(s)$, it is desired to obtain a real function of position (x, in degrees), $p(x)$, the *reconstructed field profile.* This is to be compared with the cell's *mapped field profile.* The discrete inverse Fourier transform of the following form was used, in which $x = nx_0$, $s = ks_0$, $x_0s_0 = 1/N$, and n and k take on integer values from 0 through N–1:

$$p(nx_0) = \sum_{k=1}^{N/2-1} |M(ks_0)| \cos(2\pi nk/N - \phi(ks_0)).$$

Here $\phi(s)$ is the phase of $M(s)$, i.e. $M(s) = |M(s)|\exp(-i\phi(s))$. Whereas this formula requires $M(s)$ to be known as linearly equal intervals of s, the actual studies yielded values of $M(s)$ at logarithmically equal intervals of s. It was therefore necessary to plot a smooth curve through the latter values in order to interpolate the former for use in the transform. (A typical example of this interpolation is shown in Fig. 2*A*, *B*; interpolated values for both amplitude and phase of $M(s)$ are well determined from the quarter-octave spacing of experimental values.) The constants of the calculation, x_0 and s_0, were chosen so that all significant variations in $M(s)$ were sampled, and so that values of $p(x)$ were obtained at many points x within one receptive field diameter of the cell as mapped.

The reconstructed field profile thus obtained was located with its origin at the known reference point used in phase measurement: the position of the photocell. This procedure exactly cancels the (translational) dependence of the phase function $\phi(s)$ on the position chosen for the photocell; i.e. while variations in photocell position cause $\phi(s)$ to vary, they have no effect on the final shape and absolute position of the reconstructed profile.

In some of the studies described, $\phi(s)$ was not measured, so that only $|M(s)|$ was known. In such a case, many reconstructed profiles, $p(x)$, could be derived from the selectivity curve, $|M(s)|$, as the phase function, $\phi(s)$, was varied. The phases were varied systematically to bring $p(x)$ into even closer approximation with the mapped profile. The phase function was constrained by a smoothness condition, namely, to have a slope which nowhere exceeds that of the experimentally measured phase functions of six cells. Specifically, adjacent values ($\phi(s)$ and $\phi(s+s_0)$) were permitted to differ by no more than 100 degrees. A typical set of phase values chosen is shown in Fig. 2*C*. The closest approximation attainable, at a resolution of 20–40 degrees of phase in each spatial frequency component, was that adopted as the reconstructed field profile.

RESULTS

Mapped field profile

By the use of a stationary light bar stimulus, a simple cell's field was resolved into discrete *on-regions* and *off-regions*. Another type of region was sometimes present, in which a stimulus inhibited an on-response but could not produce an off-response. These regions will be termed *weak off-regions*.

The fields of all the simple cells we studied consisted of either two or three distinct regions, including the weak regions. Stimulation beyond these regions with single bars never revealed additional zones influencing the cell's response. Of the sixteen cells

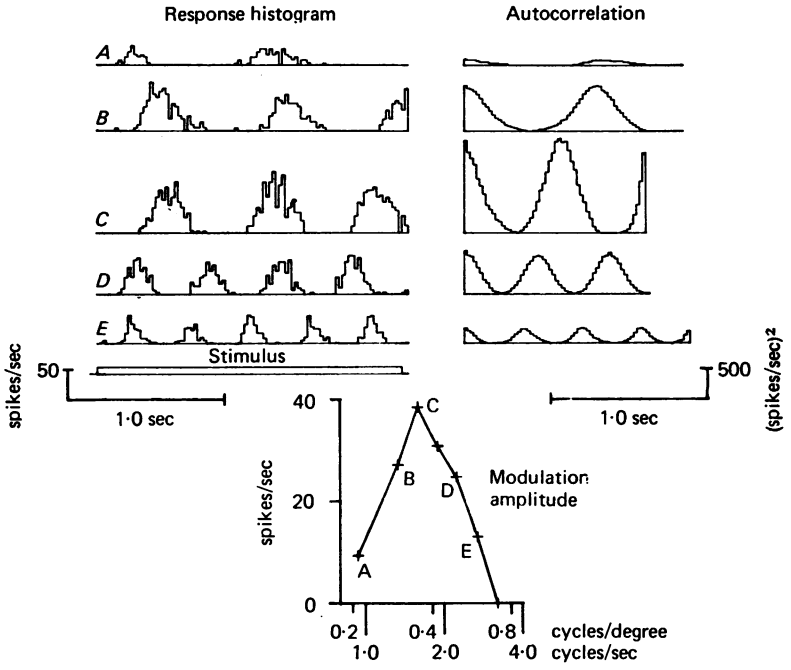

Fig. 1. Constant-velocity selectivity of cell 20–8 at velocity 4·5 degrees/sec. Each response to a moving grating (left column) is accompanied by its autocorrelation (right column). Calibrations apply to all responses and autocorrelations. Stimulus trace applies to all responses. Bottom panel shows modulation amplitude (M) of response as a function of stimulus spatial frequency and temporal frequency. Letters on plot correspond to those at left of responses. The selectivity is summarized in Table 1.

analysed in detail, four were bipartite and twelve tripartite; seven were sustained, seven transient, and two undetermined. Fields varied greatly with respect to the relative widths and strengths of their on- and off-regions. Certain tripartite fields possessed a flanking region of such weak influence that the field resembled very closely a bipartite field. Considering the great variety of field profiles among tripartite cells, it seems more accurate to regard the bipartite class as the extreme of a continuum of varying field shapes than as a distinct group. However, we will continue to use the names 'bipartite' and 'tripartite', as they do have descriptive value.

Selectivity studies with gratings

The response of a simple cell to a drifting sinusoidal grating consists of a modulated discharge at the temporal frequency of the stimulus. The modulation is truncated for approximately half of each cycle at zero firing rate (see Fig. 1). Movshon & Tolhurst (1975) aptly termed the simple cell's response wave form a 'half-wave rectified'

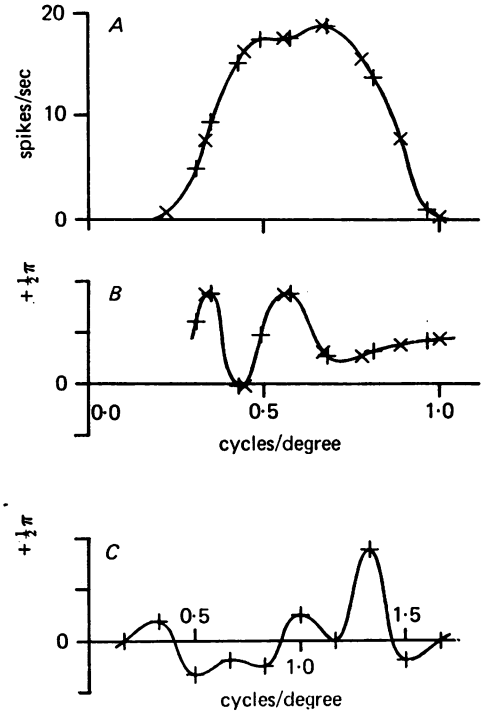

Fig. 2

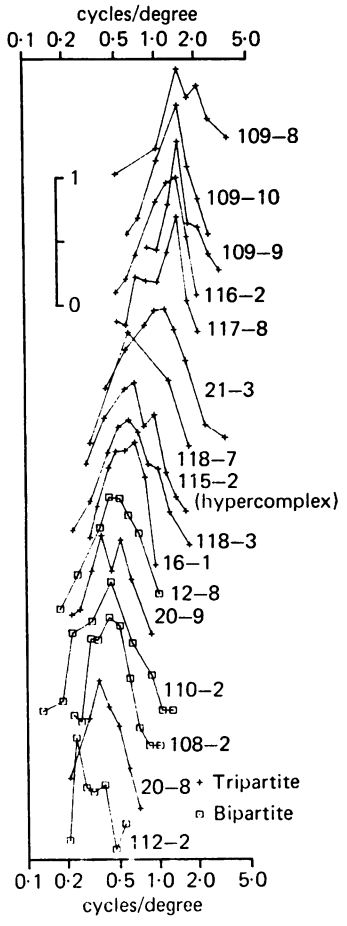

Fig. 3

Fig. 2. *A*, *B*, experimentally measured amplitude (*A*) and phase (*B*) of the responses of cell 16–1 to drifting gratings. Crosses (+) are experimental values, from which the smooth curves were drawn in order to interpolate values (×) at linear intervals of spatial frequency (see Methods). Phase is expressed in radians. *C*, values of phase adopted for a cell (118–3) of whose responses the phases were not measured (see Methods). The continuous curve is drawn for comparison with the measured phase function of cell 16–1 in *B*.

Fig. 3. Summary of constant-velocity selectivity curves of simple cells. Selectivity of modulation amplitude is plotted here. Base lines are staggered vertically to separate curves for clarity. Calibration at left shows full and half value of peak of each curve. Curves marked with squares are those of strictly bipartite cells.

sinusoid. One simple cell, 109–8, exhibited spontaneous firing. Its responses showed full modulations, the discharge rate minima subsiding well below the spontaneous rate.

The amplitudes of the responses of each simple cell to a series of gratings were measured by the autocorrelation technique described in Methods. Representative responses of a simple cell to drifting sinusoidal gratings in a constant-velocity study are shown in Fig. 1. Each response is accompanied by its autocorrelation. This cell is

TABLE 1. Results of spatial frequency selectivity studies

Cell	Constant parameter of study	Position of tuning peak	Full width at half-maximal amplitude (octaves)	Sustained, transient	Field (bi-, tri-partite)
		Constant-velocity studies			
	Degrees/sec	Cycles/degree			
109–8	1·91	1·77	1·5	S	3
109–9	0·93	1·49	0·56	S	3
117–8	2·01	1·45	1·5	S	3
116–2	2·25	1·4	1·2	S	3*
109–10	1·56	1·35	0·93	T	3
21–3	2·11	1·09	1·88	S	3
118–7	1·91	0·8	1·53	S	3
115–2 (h)	1·43	0·68	1·73	T	3*
118–3	2·39	0·61	1·57	S	3
16–1	2·83	0·61	1·30	T	3
12–8	3·67	0·47	1·65	T	2
20–9	4·49	0·43	1·45	—	3
108–2	3·54	0·42	1·1	T	2
110–2	3·71	0·40	1·58	T	2
	1·82	0·35	1·14		
20–8	4·49	0·37	1·05	—	3
112–2	5·03	0·3	1·1	T	2
		Constant-temporal-frequency studies			
	Cycles/sec	Cycles/degree			
116–2	2·72	1·22	1·44	S	3
117–8	2·65	1·22	1·5	S	3*
115–2 (h)	4·76	0·68	1·87	T	3*
118–3	5·62	0·7	1·07	S	3
	2·00	0·61	1·43		
108–2	1·49	0·37	2	T	2
110–2	1·64	0·33	1·93	T	2
112–2	2·90	0·3	0·87	T	2

(h = hypercomplex)
* Tripartite counting weak regions.

typical in that it is silent about half the time in every response, regardless of spatial frequency. The cell's peak discharge rate of over 50 spikes/sec in response to the optimal grating (Fig. 1*C*) is typical. Note the striking constancy of the half-wave rectified wave form of the response over a wide range of spatial frequency.

The spatial frequency selectivity curve of another cell appears in Fig. 2*A*, *B*. In this case both amplitude (*A*) and phase (*B*; as calculated from photocell measurements) are shown. It should be borne in mind that the form of the phase function depends not only on the cell's responses but also on the position of the photocell.

The selectivity curves for all sixteen simple cells on which complete constant-velocity studies were performed are shown in Fig. 3. The typical curve has only one peak, with a full width at half-maximal amplitude of approximately 1·3 octaves. The

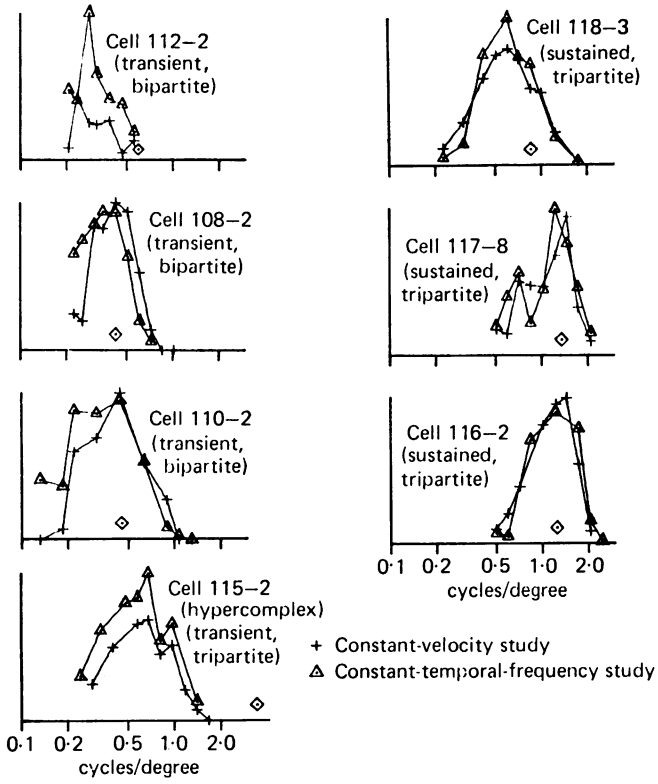

Fig. 4. Comparison of constant-velocity selectivity with constant-temporal-frequency selectivity. For each cell, the modulation amplitude is plotted as a function of spatial frequency in both a constant-velocity study (crosses) and a constant-temporal-frequency study (triangles). The two curves within each panel are plotted to the same vertical scale (spikes/sec). The diamond in each panel indicates the stimulus common to the two studies. All curves are plotted to the same horizontal scale. Transient cells are at left, sustained cells at right. Within experimental accuracy, the preferred spatial frequency of a cell does not depend on which type of study is performed.

selectivity curves share an important property: the amplitude falls to zero quite abruptly on both sides of the principal peak, and remains zero for spatial frequencies higher and lower than the respective cut-offs. (To preserve clarity, the complete cut-offs were not plotted in all cases.) Shoulders and secondary peaks appearing at the sides of principal peaks in some of the curves were not reproducible when studies were repeated at different velocities. Note the tendency of bipartite cells (squares)

as a group to prefer lower spatial frequencies than tripartite cells (crosses). Breadths and peak positions of all selectivity curves appear in Table 1.

Constant-temporal-frequency grating studies were also performed on seven of the same sixteen cells. A comparison is shown in Fig. 4 of selectivity at constant temporal frequency with selectivity at constant velocity for the seven cells. The peaks of the two selectivity curves for each cell occur at very nearly the same spatial frequency. This holds regardless of whether the spatial frequency of the stimulus common to the two studies was near the peaks. In this comparison the express preference of each cell for a certain spatial frequency is manifest. Peak positions and tuning breadths for these studies appear in Table 1.

Cell 115–2 was 'hypercomplex' as defined by Hubel & Wiesel (1965) in that its response to a moving bar was greatly reduced when the bar's length was increased beyond a critical value. However, it was also 'simple' in that the field consisted of discrete on- and off-regions. Moreover, the responses of this cell to drifting gratings and its selectivity at constant velocity and at constant temporal frequency do not in any way distinguish it from the rest of our simple cells (see Fig. 4 and Table 1).

Stationary gratings

One of the assumptions underlying the field profile reconstruction was constancy of response latency with varying spatial frequency. To test this assumption a cell was studied with stationary gratings. The contrast of the gratings was well above threshold. Each grating was flashed at ten spatial phases, uniformly distributed over one cycle. The cell responded at only two to five of the 10 phases for each spatial frequency. The spatial phase eliciting the response of greatest amplitude did so with a latency which varied by at most ± 2 msec among eight spatial frequencies spanning two octaves. This 2 msec difference was small compared to the latency of 30 msec for this cell. Other data indicate that a typical latency for a transient cell is 30 msec, and for a sustained cell, 85 msec.

Fourier transformation of selectivity curves

We consider now the relationship between the simple cell's spatial frequency selectivity and its field profile. The specific question to be addressed is whether these two functions constitute a Fourier transform pair. Each cell's constant-velocity selectivity curve was inverse Fourier transformed, and the result compared with the respective mapped field profile. For the purpose of the inverse Fourier transform, each selectivity curve was sampled on both sides of the peak well into the spatial frequency ranges of zero response.

The *mapped profile*, exactly as plotted with stationary bars during the experiment, is compared with the *reconstructed profile* in Fig. 5. The comparison is shown for eight cells representative of the sixteen cells on which we completed the analysis. In the cases of the four cells shown in the top half of the figure, the phases of the responses to gratings were known, and the reconstructed profiles were completely determined. In the other four cases (bottom half of Figure), the phases were unknown, and a 'best match' reconstructed profile was computed, as explained in Methods.

Each reconstructed profile is in qualitative agreement with the shape of the corresponding mapped profile over the domain where the mapped profile could be

mapped, i.e. where the cell was responsive to stationary light bars. The intervals in which the two functions are positive (on-region) and negative (off-region) correspond well in extent and position. A stronger statement of likeness cannot be made, since it was not possible to measure quantitatively the amplitude of the mapped profile.

An important feature of the reconstructed profiles of all cells is the presence of

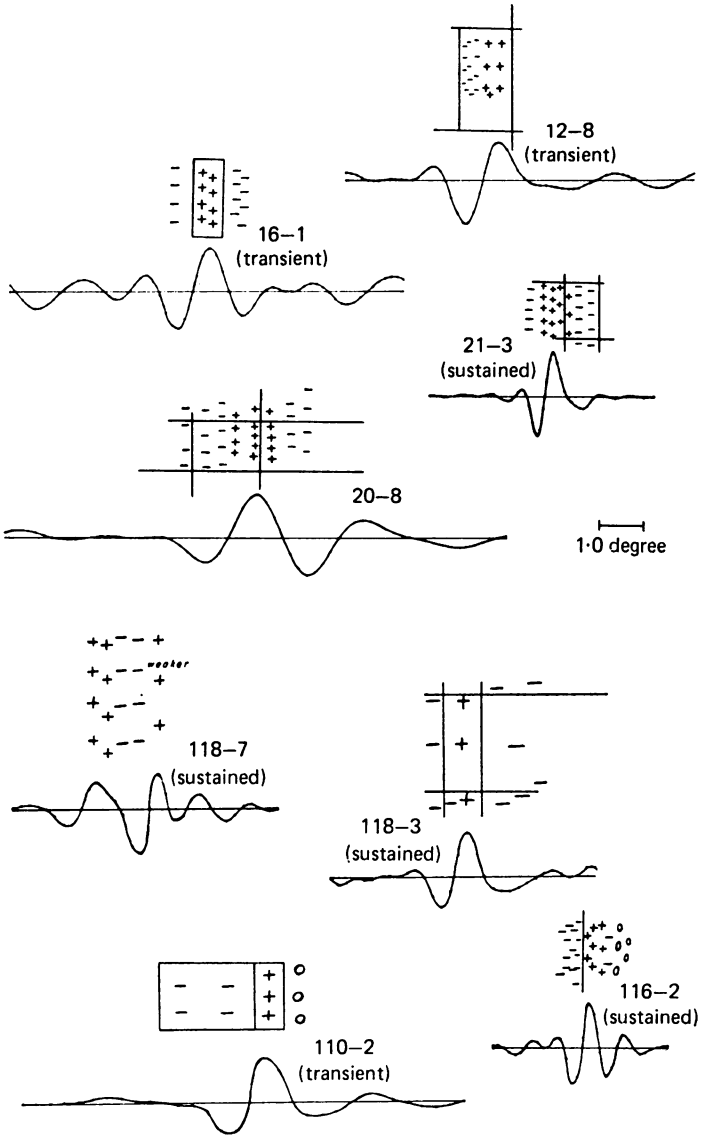

Fig. 5. Comparison of mapped field profiles with reconstructed profiles. For each cell the field is shown as mapped during the experiment (*mapped profile*); number of + or − signs in a region indicates strength of influence of a stimulus filling that region. Below each mapped profile appears the cell's *reconstructed profile*. All profiles are plotted to the same horizontal scale. All fields are arbitrarily shown with preferred orientation vertical. Examples are shown of cells with known phases (top four) and cells with unknown phases (bottom four).

significant side-lobes far from the centre of the profile, where the cell was unresponsive to stationary light bars, even upon averaging of repeated presentations. In the cases of unmeasured phases, where a phase function was constructed subject only to the constraint of qualitative agreement with the mapped profile, no adjustment of the phase function could suppress these distant side-lobes in the reconstructed profile.

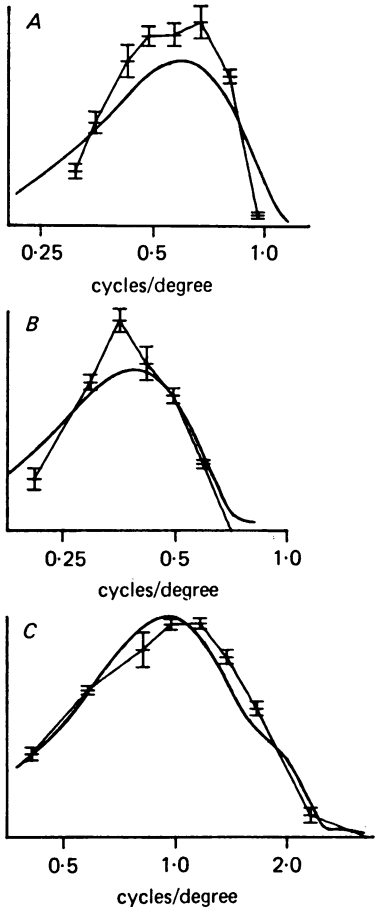

Fig. 6. Comparison of experimentally measured spatial frequency selectivity (curve with error bars) with the curve derived from suppressing the side-lobes in the reconstructed field profile. The latter curve differs greatly from the actual behaviour of the cell in *A* and *B*, and less so, but still significantly, in *C*. *A*, cell 16–1; *B*, cell 20–8; *C*, cell 21–3.

In order to evaluate the influence of the side-lobes on spatial frequency selectivity, the following comparison was made. The side-lobes (i.e. all of the reconstructed field profile lying outside the region responsive to light bars) were set to zero, and the resulting profile was transformed back to the spatial frequency domain. This yielded a modified selectivity curve which could be compared with the experimentally measured selectivity curve (see Fig. 6; standard errors appear on experimental curve). Considering the experimental error in measuring response amplitudes, the

modified curve departs significantly from the experimental curve. Where the side-lobes are prominent, the two curves differ greatly, the modified curve having smaller peak amplitude, greater full-width at half-maximal amplitude, and a more gradual low-frequency cut-off (Fig. 6*A*, *B*). Where the side-lobes are less prominent, the difference is less marked, but is still significant (Fig. 6*C*).

DISCUSSION

Truncated modulation

Every simple cell but one responded to drifting sinusoidal gratings with a half-wave rectified sinusoidal response. As noted by Schiller, Finlay & Volman (1976), this wave form is as reliable a criterion as any other for distinguishing simple and complex cells. Moreover, the simple cell differs in this respect from the periodic complex cell found within the same cortex, which generates both a fully modulated and an unmodulated component in response to drifting gratings (Pollen, Andrews & Feldon, 1978). Unlike retinal ganglion and geniculate cells, the simple cell has practically no spontaneous activity in either the presence or absence of nitrous oxide anaesthesia (Andrews, 1977). Thus, the simple cell is generally unable to signal net inhibition and does not display full modulation.

Spatial frequency selectivity

The simple cell's responses to drifting sinusoidal gratings have been examined in two types of studies. The tuning breadth (full breadth at half-maximal amplitude) in the constant-velocity studies averaged $1{\cdot}3 \pm 0{\cdot}3$ octaves, and in constant-temporal-frequency studies, $1{\cdot}5 \pm 0{\cdot}4$ octaves.

Maffei & Fiorentini (1973) showed typical constant-velocity selectivity curves of simple cells with full widths of $1{\cdot}0 \pm 0{\cdot}2$ octaves, slightly lower than the value we measured (1·3 octaves). They measured responses in terms of modulation amplitude, as we did.

The range of spatial frequencies over which simple cells have selectivity peaks is about 0·3–1·8 cycles per degree in our constant-velocity studies in the central 5 degrees of visual space (see Fig. 3), in agreement with the findings of Maffei & Fiorentini (1973). The extent of this range, about three octaves, is comparable to the range of receptive field sizes found by Hubel & Wiesel (1962) near the centre of gaze, 0·5 to 6 degrees. The range of simple cell selectivity peaks found by Ikeda & Wright (1975) in constant-temporal-frequency studies is 0·3–2·0 cycles/degree, with one additional cell peaking at 2·8 cycles/degree.

Fourier reconstruction of field profile

The Fourier transform is an operation embodying linear summation of sinusoidal components. Therefore, the extent to which the Fourier transform successfully describes the relationship between the selectivity of a simple cell's responses to sinusoidal stimuli and its field profile reflects the extent to which the cell performs linear spatial summation.

For the purpose of Fourier transforming a simple cell's spatial frequency selectivity curve for comparison with the mapped field profile, either the selectivity at constant

velocity or at constant temporal frequency could have been used. In the absence of exhaustive selectivity studies covering broad ranges of velocity, temporal frequency, and spatial frequency, it is not clear which curve, if either, is the more fundamental indication of the cell's spatial filtering properties. However, when an arbitrary stimulus is presented to the cell, it passes across the receptive field with all of its spatial frequency components moving at the same velocity. The activity of the cell will therefore reflect its relative sensitivity to the various components at constant velocity. Consequently, the constant-velocity curves were used for Fourier transformation.

The comparison of mapped with reconstructed profiles will be considered separately over two domains: (1) the classical receptive field, in which the mapped profile is non-zero, i.e. in which the simple cell is responsive to stationary light bars; (2) the domain external to (1).

Within the domain in which the cell is responsive to stationary bars, the reconstructed profile shows qualitative agreement with the mapped profile. By this we mean that while comparison of the amplitudes of the two functions could not be made quantitatively, the intervals over which they have the same sign correspond well in width and position.

Two groups of cells will be considered. In the case of the cells whose selectivity curves include phase information, not only the *shape* but also the absolute *position* of the reconstructed profile is determined by the known phases. There is qualitative agreement with the shape of the mapped profile. A small discrepancy appeared in the position which could be explained by a uniform latency in the cell's responses to all gratings. Our complete study of one simple cell using stationary gratings revealed that the latencies are indeed uniform among gratings. Abbreviated studies of other cells indicated that the latency of a cell's response to stationary stimuli accounted well for the discrepancy in position of the reconstructed profile. The mapped and reconstructed profiles therefore agree qualitatively in both shape and position.

In the case of the cells whose selectivity curves were measured without phase information, the phases were systematically varied to produce a reconstructed profile resembling as closely as possible the mapped profile. In general one set of phases could be found yielding a best match to the mapped profile. In most cases a resemblance could be achieved which was as close as that found for the cells with known phases.

Outside the area of its field where a cell was responsive to stationary bars, the reconstructed profile displays side-lobes of significant amplitude. No adjustment of the phases of the values in the selectivity curve could suppress these distant side-lobes in the reconstructed profile. This is understandable in terms of a fundamental principle of the Fourier transform: the more abrupt are the changes in a function, the greater must be the strength of its Fourier transform far from the origin. Thus, it is the sharpness of the simple cell's selectivity curve and the abruptness with which it falls to and remains at zero that require significant side-lobes far from the origin in the reconstructed profile. This principle was the basis for MacLeod & Rosenfeld's statement (1974) that a tuning band width of about an octave requires the field to have 'a spatial extent of at least a couple of cycles'.

The existence of side-lobes in the reconstructed profile might appear inconsistent

with the mapped profile, which shows no activity elicited by stationary bars flashed at these positions. However, this apparent discrepancy may indicate the existence of active regions far from the centre of the field which simply do not excite the cell above threshold when stimulated alone. This indication of side lobes is consistent with the demonstration by Maffei & Fiorentini (1976) of 'unresponsive regions' at the periphery of the simple cell field which can strongly facilitate or inhibit the cell's response. Moreover, the qualitative agreement of reconstructed and mapped profiles in the responsive regions is consistent with the possibility of linear spatial summation across the receptive field of the simple cell.

We thank Ms Judy Levy and Mr Peter Bridgman for their excellent technical assistance. We are very grateful to Drs Whitman Richards and Richard Kronauer for their suggestions and criticisms. This investigation was supported by U.S. Public Health Service Research Grant EY 00597 from the National Eye Institute. B.W.A. was supported in part by a National Science Foundation Graduate Fellowship.

REFERENCES

ANDREWS, B. W. (1977). Spatial frequency tuning of striate cortical neurons in cat and its relation to receptive field profile. Doctoral thesis, Harvard University, Cambridge, Massachusetts, U.S.A.

BISHOP, P. O., COOMBS, J. S. & HENRY, G. H. (1971). Responses to visual contours: spatio-temporal aspects of excitation in the receptive fields of simple striate neurones. *J. Physiol.* **219**, 625–657.

BISHOP, P. O., HENRY, G. H. & SMITH, C. J. (1971). Binocular interaction fields of single units in the cat striate cortex. *J. Physiol.* **216**, 39–68.

CAMPBELL, F. W., COOPER, G. F. & ENROTH-CUGELL, C. (1969). The spatial selectivity of the visual cells of the cat. *J. Physiol.* **203**, 223–235.

FRIES, W. & ALBUS, K. (1976). Static and dynamic properties of receptive fields of some simple cells in cat's striate cortex. *Vision Res.* **16**, 563–566.

HUBEL, D. H. (1957). Microelectrode for recording from single cells. *Science, N.Y.* **125**, 549–550.

HUBEL, D. H. & WIESEL, T. N. (1962). Receptive fields, binocular interaction, and functional architecture in the cat's visual cortex. *J. Physiol.* **160**, 106–154.

HUBEL, D. H. & WIESEL, T. N. (1965). Receptive fields and functional architecture in two nonstriate visual areas (18 and 19) of the cat. *J. Neurophysiol.* **28**, 229–289.

IKEDA, H. & WRIGHT, M. J. (1974). Evidence for 'sustained' and 'transient' neurones in the cat's visual cortex. *Vision Res.* **14**, 133–136.

IKEDA, H. & WRIGHT, M. J. (1975). Spatial and temporal properties of 'sustained' and 'transient' neurones in area 17 of the cat's visual cortex. *Exp. Brain Res.* **22**, 363–383.

MACLEOD, I. D. G. & ROSENFELD, A. (1974). The visibility of gratings: spatial frequency channels or bar-detecting units? *Vision Res.* **14**, 909–915.

MAFFEI, L. & FIORENTINI, A. (1973). The visual cortex as a spatial frequency analyzer. *Vision Res.* **13**, 1255–1267.

MAFFEI, L. & FIORENTINI, A. (1976). The unresponsive regions of visual cortical receptive fields. *Vision Res.* **16**, 1131–1139.

MOVSHON, J. A. & TOLHURST, D. J. (1975). On the response linearity of neurones in cat visual cortex. *J. Physiol.* **249**, 56–57*P*.

POLLEN, D. A., ANDREWS, B. W. & FELDON, S. E. (1978). Spatial frequency selectivity of periodic complex cells in the visual cortex of the cat. *Vision Res.* **18**, 665–682.

POLLEN, D. A. & RONNER, S. F. (1975). Periodic excitability changes across the receptive fields of complex cells in the striate and parastriate cortex of the cat. *J. Physiol.* **245**, 667–697.

SCHILLER, P. H., FINLAY, B. L. & VOLMAN, S. F. (1976). Quantitative studies of single-cell properties in monkey striate cortex. III. Spatial frequency. *J. Neurophysiol.* **39**, 1334–1351.

STROMEYER, C. F. III, LANGE, A. F. & GANZ, L. (1973). Spatial frequency phase effects in human vision. *Vision Res.* **13**, 2345–2359.